Few-optical-cycle Bessel-Gauss pulsed beams in free space

M. A. Porras
Departamento de Física Aplicada, Escuela de Ingenieros de Minas, Universidad Politécnica de Madrid, Rios Rosas 21, E-28003 Madrid, Spain

R. Borghi
Dipartimento di Ingegneria Elettronica, Università degli Studi Roma Tre and Istituto Nazionale per la Fisica della Materia, Via della Vasca Navale 84, I-00146 Rome, Italy

M. Santarsiero
Dipartimento di Fisica, Università degli Studi Roma Tre and Istituto Nazionale per la Fisica della Materia, Via della Vasca Navale 84, I-00146 Rome, Italy

(Received 7 February 2000; revised manuscript received 19 May 2000)

We introduce a new family of nonseparable, pulselike and beamlike solutions of the wave equation in the paraxial approximation with pseudonondiffracting behavior. They are the pulsed versions of the Bessel-Gauss beams by Gori *et al.*, and encompass as particular cases the diffraction-free Bessel-*X* pulses, isodiffracting pulses, and, in the many-cycle limit, Bessel and Gaussian beams. Unlike Bessel-*X* waves, these solutions carry finite energy but retain nondiffracting behavior over a finite propagation distance, and could be physically produced with mode-locked toroidal resonators.

PACS number(s): 42.25.−p, 42.65.Re, 42.65.Sf

I. INTRODUCTION

Recent developments in laser technology have resulted in the generation of extremely short and intense laser pulses, containing only a few field oscillations, even only one, at optical frequencies [1]. Much attention is therefore being paid to the problem of their propagation in vacuum [2,3], dispersive linear [4] and nonlinear media [1,5], optical systems [6,7], and in particular to their diffraction properties, which have been shown to differ substantially from those of quasimonochromatic, many-cycle pulses. For ultrashort pulses, due to the ultrawide frequency spectra involved, diffraction appears like a dispersive phenomenon [8,9], in the sense that the dependence of diffraction on frequency cannot be neglected. Among the numerous studies on diffraction of few-cycle pulses, a number of papers [3,10–15] report model solutions of the propagation equations, both in the paraxial and nonparaxial regimes, from which many distinctive features of their propagation have been inferred.

Isodiffracting (ID) pulses [6,16], for instance, also called pulsed Gaussian beams [3,11], are superpositions of Gaussian beams with different frequencies and a common Rayleigh range. They appear to be the simplest nontrivial model for pulsed-beam propagation, since they already contain some spatiotemporal coupling phenomena arising from dispersive diffraction, such as time differentiation on propagation, temporal and spectral changes along the transversal plane, and time-dependent diffraction [3,11]. ID pulses carry finite energy and appear to be an adequate model for the radiation from mode-locked lasers with stable two-mirror resonators.

Bessel-*X* waves [13–15], on the other hand, are superpositions of Durnin's Bessel beams [17] with different frequencies. They represent a class of pulsed beams with optimum propagation properties, since they are diffraction- and dispersion-free, i.e., they maintain their transversal and longitudinal localization upon propagation over arbitrary distances. Unfortunately, the Bessel-*X* waves carry infinite energy, like monochromatic Bessel beams, and therefore are not physically realizable.

In this paper, we introduce a class of pulsed beams, obtained as superpositions of Bessel-Gauss (BG) beams [18,19]. BG beams were introduced by Gori *et al.* [19] as the paraxially propagated field of a Bessel function apertured by a Gaussian distribution. They are therefore finite-energy, physically realizable versions of the Bessel beam, simulating the nondiffracting behavior of the latter over a certain propagation distance [19]. Apart from their appealing analytical properties and propagation features, BG beams have found application in resonator theory [20], and very recently in nonlinear optics [21,22] for improving the efficiency of second-order harmonic generation. Suitably superposing BG beams of different frequencies, we construct pulsed-beam solutions of the paraxial wave equation, which will be termed BG pulsed beams.

In particular, the BG pulsed beams with the so-called Poisson-like [3] or ''power spectrum'' [12], which is often used to model few-cycle pulses, lead to a four-parameter family of nonseparable pulsed-beam solutions of the paraxial wave equation in terms of Legendre polynomials. This type of BG pulsed beam encompasses the ID pulses and the Bessel-*X* waves as particular cases and, in the many-cycle limit, BG beams, and hence Gaussian and Bessel beams.

We show that few-cycle BG pulsed beams can present pseudo-non-diffracting behavior for suitable choices of their parameters. This means that they imitate the nondiffracting behavior of *X*-Bessel waves over a finite propagation distance, or diffraction-free range, which is shown to be larger than the diffraction length expected from its transversal size. At the same time, BG pulsed beams retain the property of ID pulses of carrying a finite amount of energy, i.e., of being physically realizable. We show, indeed, that BG pulsed beams can model the output radiation from stable mode-locked toroidal resonators.

II. PROPAGATION EQUATIONS AND BASIC SOLUTIONS

We begin our analysis by considering a linearly polarized light beam with field $E(\mathbf{x}_\perp, z, t)$, $\mathbf{x}_\perp \equiv (x,y)$, propagating along the positive z direction according to the wave equation

$$\Delta E - \frac{1}{c^2}\frac{\partial^2 E}{\partial t^2} = 0, \tag{1}$$

where Δ denotes the Laplacian operator. It is convenient to introduce the local coordinates $t' = t - z/c$, $z' = z$, to extract from E its rapid variation along z due to the wave transport at the velocity c. Then the remaining dependence of $E(\mathbf{x}_\perp, z', t')$ on the new propagation coordinate z' describes only changes due to diffraction, i.e., to the finite transversal extent of the wave. For a paraxial wave, one can assume that these changes are slow enough so that $|\partial E/\partial z'| \ll (1/c)|\partial E/\partial t'|$, or equivalently, $\Delta z \gg c\Delta t$, where Δz and Δt are typical length and variation time of $E(\mathbf{x}_\perp, z', t')$. To fix ideas, we can think of Δz as the diffraction length and Δt as a suitable fraction of the period T_0 in the case of a pulse with a few oscillations, e.g., $T_0/2\pi = 1/\omega_0$, corresponding to a phase increase of 1 rad. Taking the following relations into account:

$$\frac{\partial}{\partial z} = \frac{\partial}{\partial z'} - \frac{1}{c}\frac{\partial}{\partial t'},$$

$$\frac{\partial}{\partial t} = \frac{\partial}{\partial t'},$$

and performing the above approximation, the wave equation (1) transforms into

$$\frac{2}{c}\frac{\partial^2 E}{\partial t' \partial z'} = \Delta_\perp E, \tag{2}$$

where $\Delta_\perp$ is the two-dimensional Laplace operator perpendicular to the propagation direction. This equation is presently receiving much attention [2,3,8,9] since it allows one to extend the simple paraxial treatment of diffraction to arbitrary ultrashort waveforms.

A fundamental solution of Eq. (2) is, of course, the monochromatic Gaussian beam

$$E(r,z,t) = \frac{iz_0}{q}\exp\left(-\frac{i\omega r^2}{2cq}\right)\exp(i\omega t'), \tag{3}$$

where ω is the angular frequency of light, $r^2 = x^2 + y^2$, $q = z + iz_0$, and $z_0 > 0$ is the Rayleigh range or diffraction length. (Note that we omit the prime sign in z in integrated expressions, since numerically $z' = z$.) Pulsed-beam solutions of Eq. (2) can now be constructed by suitably superposing Gaussian beams. For example, the superposition

$$E(r,z,t) = \frac{iz_0}{q}\frac{1}{\pi}\int_0^\infty d\omega\, \hat{f}(\omega)\exp\left(-\frac{i\omega r^2}{2cq}\right)\exp(i\omega t') \tag{4}$$

of Gaussian beams with different frequencies ω but with the same Rayleigh range z_0 results in the ID pulse [6,16], or pulsed Gaussian beam [3,11],

$$E(r,z,t) = \frac{iz_0}{q}F\left(t' - \frac{r^2}{2cq}\right), \tag{5}$$

where

$$F(t) = \frac{1}{\pi}\int_0^\infty d\omega\, \hat{f}(\omega)\exp(i\omega t) \tag{6}$$

is the analytic signal of the real pulse shape $f(t) = \mathrm{Re}[F(t)]$. The spot size of the ID pulses increases on propagation according to the hyperbolic law [3] $a(z) = a_0\sqrt{1 + z^2/z_0^2}$, from a waist or minimum width $(z=0)$ of the order of

$$a_0 \sim \sqrt{2c\Delta t z_0}, \tag{7}$$

with Δt the typical variation time of $F(t)$, up to $a(z) = z\theta_0$ in the far field $(z \gg z_0)$, where the divergence angle is approximately given by

$$\theta_0 \sim \sqrt{2c\Delta t/z_0}. \tag{8}$$

The spreading properties of the ID pulses thus closely resemble those of each Gaussian beam in the superposition, due to their common Rayleigh range z_0.

On the other hand, superpositions of Bessel beams of the form

$$E(r,z,t) = \frac{1}{\pi}\int_0^\infty d\omega\, \hat{f}(\omega) J_0\left(\frac{\omega}{c} r \sin\theta\right)\exp(i\omega t''), \tag{9}$$

with $t'' = t - z\cos\theta/c$, of different frequencies and a common cone angle θ, lead to the nondiffracting, nondispersing X-Bessel waves [13–15], which are infinite-energy solutions of the nonparaxial wave equation (1). X-Bessel waves can alternatively be seen as superpositions of plane pulses $F(t)$ with propagation directions evenly distributed over the surface of a cone of apex angle θ. The meridian sections of the X-Bessel waves resemble a letter ''X'' of minimum width (i.e., the waist of the ''X'')

$$a_X \sim \frac{2c\Delta t}{\theta}, \tag{10}$$

propagating without deformation at the superluminal velocity $c/\cos\theta$.

III. BESSEL-GAUSS PULSED BEAMS

A. Frequency-domain analysis

To combine the nondiffracting properties of X-Bessel waves with the finite energy of the ID pulses, we replace both the Gaussian and the Bessel basis with the monochromatic BG family of solutions of the paraxial wave equation (2), namely [19],

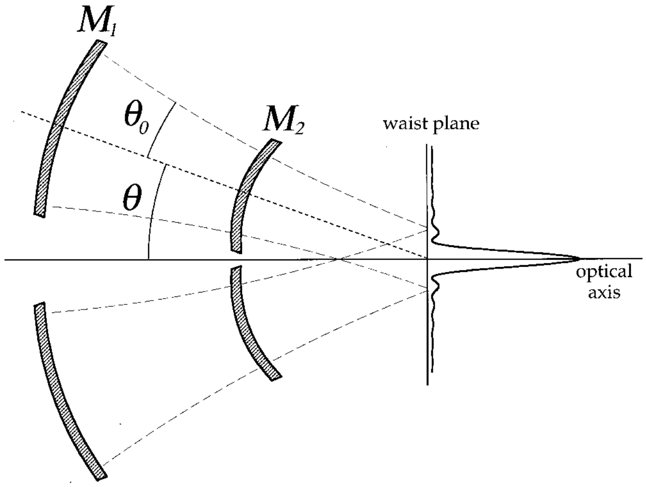

FIG. 1. Sketch of a stable toroidal resonator to generate the BG pulsed beam.

$$E(r,z,t)=\frac{iz_0}{q}\exp\left[-\frac{i\omega}{2cq}(r^2+z^2\theta^2)\right]\times J_0\left(\frac{iz_0}{q}\frac{\omega}{c}\theta r\right)\exp(i\omega t''), \tag{11}$$

where now

$$t''=t-z(1-\theta^2/2)/c=t'+z\theta^2/2c \tag{12}$$

is the paraxial approximation of the reduced time t'' in the expression of the X-Bessel waves [Eq. (9)], and $J_0(\,)$ is the zero-order Bessel function of the first kind [23]. Of course, there are other possibilities to bring together nondiffracting behavior and finite energy. The Bessel function can be apertured, for example, with a super-Gaussian window [24], or a hard-edged aperture [25], but contrary to the Gaussian window, these choices do not lead to an analytic expression for the propagated field.

New pulsed-beam solutions of the paraxial wave equation (2) can now be constructed by superposing BG beams of different frequencies, i.e.,

$$E(r,z,t)=\frac{iz_0}{q}\frac{1}{\pi}\int_0^\infty d\omega\,\hat{f}(\omega)\exp\left[-\frac{i\omega}{2cq}(r^2+z^2\theta^2)\right]\times J_0\left(\frac{iz_0}{q}\frac{\omega}{c}\theta r\right)\exp(i\omega t''), \tag{13}$$

where, as in the case of ID pulses and X-Bessel waves, the parameters z_0 and θ will be chosen to be independent of frequency. The remainder of this paper is devoted to the study of this kind of superposition. As we shall see later on, for specific choices of the spectrum $\hat{f}(\omega)$ or the pulse form $F(t)$, closed-form analytic expressions for Eq. (13) in terms of the Legendre polynomials can be obtained.

The construction of BG pulsed beams as a superposition of BG beams with constant Rayleigh range and apex angle suggests a possible method to experimentally produce them. According to Sheppard and Wilson [18], the BG beams can be identified as the fundamental modes of a suitably designed toroidal resonator [18,26,27]. Figure 1 shows a sketch of the meridian section of such a resonator, whose fundamental mode is a cw BG beam with certain Rayleigh range z_0 and apex angle θ. It should be stressed that these two parameters are independent of the wavelength of the BG mode, since they are fixed only by the resonator geometry. Thus, by coherently superposing cw BG fundamental modes at different frequencies, e.g., by mode-locking them inside the toroidal resonator, a BG pulsed beam of the type of Eq. (13) will be generated.

B. Time-domain analysis

The BG pulsed beam can also be constructed as a suitable superposition of pulsed spherical waves radiated by complex point sources. This alternative derivation of Eq. (13) provides a new view of the BG pulsed beams and their relationship with ID pulses and X-Bessel waves. Consider first the pulsed spherical wave from a point source at the origin of coordinates $E(\rho,t)=(1/2\pi\rho)F(t-\rho/c)$, where $\rho=(x^2+y^2+z^2)$. Under suitable complex time and axial shifts, $t\to t+i\tau_0$, $z\to q=z+iz_0$, the spherical wave remains a solution of the nonparaxial wave equation (1), and transforms into the pulsed beams from stationary complex point sources studied by Heyman, Felsen, and others in Refs. [10] and [28]. The paraxial approximation of the pulsed spherical wave

$$E(\mathbf{x}_\perp,z,t)=\frac{1}{2\pi z}F\left(t'-\frac{x^2+y^2}{2cz}\right), \tag{14}$$

satisfying the paraxial wave equation (2), transforms, under the same complex shifts, into the ID pulse,

$$E(\mathbf{x}_\perp,z,t)=\frac{1}{2\pi}\frac{iz_0}{q}F\left(t'+i\tau_0-\frac{x^2+y^2}{2cq}\right). \tag{15}$$

It has been recently shown [29] that an additional complex shift in the transversal coordinates amounts to a beam rotation. In particular, the shifts $x\to x-iz_0\theta\cos\phi$, $y\to y-iz_0\theta\sin\phi$ lead to an ID pulse whose propagation direction forms an angle θ (small enough) with respect to the z axis and an azimuthal angle ϕ with respect to the x axis. The superposition

$$E(r,z,t)=\frac{1}{2\pi}\frac{iz_0}{q}\int_0^{2\pi}d\phi\,F\left[t'+i\tau_0-\frac{(x-iz_0\theta\cos\phi)^2+(x-iz_0\theta\sin\phi)^2}{2cq}\right] \tag{16}$$

of identical ID pulses with directions evenly distributed over the surface of a cone of angle θ can be proved to be identical to the expression of BG pulsed beams [Eq. (13)]. To verify this statement, we first introduce polar coordinates, $x=r\cos\varphi$, $y=r\sin\varphi$, and let $\tau_0=-\theta^2 z_0/2c$, to write Eq. (16) as

$$E(r,z,t)=\frac{1}{2\pi}\frac{iz_0}{q}\times\int_0^{2\pi}d\phi F\left[t'-\frac{r^2+z^2\theta^2-2irz_0\theta\cos(\phi-\varphi)}{2cq}\right]. \tag{17}$$

Then, using Eq. (6) for $F(t)$ and the following integral representation of the Bessel function [23],

$$J_0(s)=\frac{1}{2\pi}\int_0^{2\pi}d\sigma\exp(is\cos\sigma), \tag{18}$$

Eq. (13) is easily recovered. We then conclude that a BG pulsed beam is a homogeneous superposition of ID pulses, all with the same Rayleigh range z_0 and waist position $z=0$, whose propagation directions are distributed over a cone of apex angle θ. An analogous scheme is used for X-Bessel waves, which are obtained by superposing plane pulses with propagation directions over a cone.

IV. BESSEL-GAUSS PULSED BEAMS WITH POISSON-LIKE SPECTRUM

We are mainly interested in the propagation features of BG pulsed beams with few optical oscillations. To this aim, the so-called Poisson-like or "power spectrum"

$$\hat{f}(\omega)=\frac{\pi t_0^\alpha}{\Gamma(\alpha)}\omega^{\alpha-1}\exp(-\omega t_0),\quad \omega>0, \tag{19}$$

$\alpha=1,2,...,t_0>0$, which has often been used for pulse and pulsed-beam modeling [3,12], appears to be particularly suitable.

The usefulness of the Poisson-like spectrum in Eq. (19) lies, first, in the fact that it yields the family of analytic pulses

$$F(t)=\frac{1}{\pi}\int_0^\infty d\omega\,\hat{f}(\omega)\exp(i\omega t)=\left(\frac{it_0}{t+it_0}\right)^\alpha, \tag{20}$$

having a characteristic rise time

$$\Delta t\sim t_0/\alpha, \tag{21}$$

a growing number of oscillations, from one-half ($\alpha=1$) to an arbitrary high number ($\alpha\to\infty$), of mean frequency [3]

$$\omega_m\simeq\alpha/t_0, \tag{22}$$

and a pulse duration [3]

$$T\simeq\sqrt{2/\alpha}\,t_0. \tag{23}$$

Pulses of the desired frequency and number of oscillations can then be tailored by suitably selecting the parameters α and t_0. Moreover, taking the limit $\alpha\to\infty$, $t_0\to\infty$, with $\alpha/t_0=\omega_m=$const, $F(t)$ tends to the monochromatic signal $\exp(i\omega_m t)$, a property which follows from the basic relation

$$\lim_{n\to\infty}(1+x/n)^n=e^x. \tag{24}$$

Second, the superposition of BG beams [Eq. (13)] with the Poisson-like spectrum, or alternatively, the superposition of ID pulses [Eq. (17)] with the analytic signal Eq. (20), can be evaluated in closed form. Using the integrals 6.621.1 or 3.661.4 of Ref. [30], we obtain

$$E(r,z,t)=\frac{iz_0}{q}\left\{\frac{it_0}{\left[(t_c+it_0)^2-\left(\frac{iz_0}{cq}\theta r\right)^2\right]^{1/2}}\right\}^\alpha\times P_{\alpha-1}\left\{\frac{t_c+it_0}{\left[(t_c+it_0)^2-\left(\frac{iz_0}{cq}\theta r\right)^2\right]^{1/2}}\right\}, \tag{25}$$

where

$$t_c=t''-\frac{1}{2cq}(r^2+z^2\theta^2) \tag{26}$$

is a space-dependent complex time, and $P_n(\,)$ is the Legendre polynomial of order n [23]. Equation (25) is a novel, four-parameter family of solutions of the paraxial wave equation having beam and pulse form. In fact, inspection of Eq. (25) shows that (a) the denominator $\{(t_c+it_0)^2-[(iz_0/cq)\theta r]^2\}$ is different from zero for any permissible value of the parameters $t_0>0$, $z_0>0$, $\theta\geqslant 0$; (b) along the transversal direction the amplitude approaches zero as $1/r^{2\alpha}$, and then the intensity as $1/r^{4\alpha}$; (c) for large values of $|t''|$, the amplitude decays as $1/|t''|^\alpha$, and then the intensity as $1/|t''|^{2\alpha}$. Therefore, (d) the integration of the intensity in time and space yields, for any value of α, a finite value of the total energy. In conclusion, Eq. (25) is a nonsingular, beamlike and pulselike, finite-energy solution of the paraxial wave equation, which moreover is endowed with pseudo-nondiffracting properties, as we shall see in Sec. VI.

V. PARTICULAR AND LIMITING CASES

One of the most appealing features of the BG pulsed beams with the Poisson-like spectrum [Eq. (25)] is its capability of reproducing light waves as Gaussian, Bessel beams, and their pulsed versions, ID and X-Bessel waves, by means of a single algebraic function.

A. Isodiffracting pulsed beams and Gaussian beams

When the cone angle is $\theta=0$, we have $t_c=t'-r^2/2cq$ and the argument of the Legendre polynomial $P_{\alpha-1}$ becomes 1, so that Eq. (25) reduces to

$$E(r,z,t)=\frac{iz_0}{q}\left(\frac{it_0}{t'-r^2/2cq+it_0}\right)^\alpha, \tag{27}$$

which is the expression of the ID pulse with the Poisson-like spectrum [3]. Furthermore, it has been proved [3] that Eq. (27) with $\alpha=1$ is the paraxial form of Ziolkowski's EDEPT (electromagnetic directed-energy pulse train) [12], and that the limit for α, $t_0\to\infty$ with $\alpha/t_0=\omega_m=$const is the monochromatic Gaussian beam of frequency ω_m.

B. Nondiffracting *X*-Bessel pulses and Bessel beams

In the limit $z_0 \to \infty$, we have $iz_0/q \to 1$, $1/q \to 0$, and $t_c \to t''$. The BG pulsed beam in Eq. (25) takes then the form of the superluminal, nondiffracting, and nondispersing Bessel-*X* pulse, that is,

$$E(r,z,t) = \left\{ \frac{it_0}{[(t''+it_0)^2 - \theta^2 r^2/c^2]^{1/2}} \right\}^{\alpha} \times P_{\alpha-1} \left\{ \frac{t''+it_0}{[(t''+it_0)^2 - \theta^2 r^2/c^2]^{1/2}} \right\}, \quad (28)$$

described by Friberg *et al.* [13]. The particular case of Eq. (28) with $\alpha=1$ is the earlier broadband *X* wave introduced by Lu and Greenleaf in Ref. [14], and the limit α, $t_0 \to \infty$ with $\alpha/t_0 = \omega_m = \text{const}$ is the monochromatic Bessel beam of Durnin *et al.* [17]. To prove formally the latter assertion, we write the denominator in the first factor of Eq. (28) as $(t''+it_0)^2 - (\theta r/c)^2 = (t''+it_0+\theta r/c)(t''+it_0-\theta r/c)$. On replacing t_0 with α/ω_m and by using Eq. (24), we get

$$\lim_{\alpha, t_0 \to \infty} \left\{ \frac{it_0}{[(t''+it_0)^2 - \theta^2 r^2/c^2]^{1/2}} \right\}^{\alpha} = e^{i\omega_m t''}. \quad (29)$$

Furthermore, on writing the argument of $P_{\alpha-1}$ in Eq. (28) as $\cos\{\tan^{-1}[(i\theta r/c)/(t''+i\alpha/\omega_m)]\}$, which for large α can be replaced by $\cos(\theta r \omega_m/\alpha c)$, and using the limiting expression $\lim_{n\to\infty} P_n[\cos(x/n)] = J_0(x)$ in Ref. [23], we obtain

$$\lim_{\alpha, t_0 \to \infty} P_{\alpha-1} \left\{ \frac{t''+it_0}{[(t''+it_0)^2 - \theta^2 r^2/c^2]^{1/2}} \right\} = J_0\left(\frac{\omega_m}{c} \theta r \right). \quad (30)$$

In conclusion, from Eqs. (29) and (30), the *X*-Bessel pulse in Eq. (28) tends to the Bessel beam $J_0(\omega_m \theta r/c)\exp(i\omega_m t'')$ as α and t_0 tend to infinity while their quotient remains constant.

C. Pseudo-non-diffracting Bessel-Gauss beams

For $\theta \neq 0$, $z_0 \neq \infty$, in the limit α, $t_0 \to \infty$ with $\alpha/t_0 = \omega_m = \text{const}$, expression (25) of the BG pulsed beam yields the expression (11) of the monochromatic BG beam of frequency ω_m. The limiting procedure to be used is similar to the one above, therefore we will not go into details.

VI. PROPAGATION FEATURES OF THE BESSEL-GAUSS PULSED BEAMS

The spatiotemporal-temporal form of the BG pulsed beams resembles in some aspects that of the Bessel-*X* pulses and in other aspects that of the ID pulses, in the same way as the cw BG beams share their propagation features with both Bessel and Gaussian beams [19].

The overall characteristics of a BG pulsed beam of parameters z_0, θ and temporal form $F(t)$ can be easily inferred from its representation in terms of a superposition of ID pulses of the same value of z_0, pulse form $F(t)$, and propagation directions over a cone of angle θ. When θ is significantly smaller than the spreading angle of the ID pulses, θ_0, one can expect the superposition not to differ substantially from a single ID pulse, that is, from the limiting case of $\theta = 0$. On the contrary, when θ is larger than θ_0, the component ID beams will overlap only up to a finite axial distance. Within such a distance, the superposition is expected to resemble the Bessel-*X* wave of cone angle θ, since such a superposition can be assimilated, up to a certain extent, to a conical superposition of plane pulses, as is the case of the Bessel-*X* pulses. The axial distance where the ID pulses keep on overlapping, or diffraction-free range *D*, can be estimated [19] as the propagation distance at which a typical tilted ID pulse in the superposition shifts transversally for a distance equal to its transversal width a_0, that is, $D = a_0/\theta$, or on account of Eq. (7), $D \sim \sqrt{2c\Delta t z_0}/\theta$, which gives an estimate of the diffraction-free range in terms of the BG pulsed-beam characteristics. In the case of the BG pulsed beam with the Poisson-like spectrum, we obtain

$$D \sim \left(\frac{2ct_0 z_0}{\alpha \theta^2} \right)^{1/2}. \quad (31)$$

On defining a fictitious ''equivalent'' diffraction length of the Bessel-*X* wave according to the transversal width as $z_X = k_m a_X^2/2 = \omega_m a_X^2/2c = \alpha a_X^2/2ct_0$, and using that from Eqs. (10) and (21) $a_X \sim 2ct_0/\alpha\theta$, we obtain the expression $D \sim \sqrt{z_X z_0}$, that is, the diffraction-free range is approached by the geometric mean of the diffraction lengths of the limiting ID and Bessel-*X* waves and, in particular, the diffraction-free range *D* is always larger than the diffraction length z_X expected from its transversal width.

The above considerations are sustained by numerical use of the expression (25). Figure 2(a) shows the real part of the field *E* of the BG pulsed beam with the Poisson-like spectrum and with a typical set of parameters ($z_0 = 18$ mm, $\theta = 0.025$ rad, $\alpha = 6$, $t_0 = 18$ fs) when it is centered at $z=0$, i.e., at the real time $t=0$. The pulse form consists of about one-and-a-half oscillations of wave number ω_m/c, with the frequency $\omega_m = \alpha/t_0 = 3\ \text{fs}^{-1}$. The divergence angle of the composing ID pulses is given by $\theta_0 = \sqrt{2ct_0/z_0\alpha} = 0.01$ rad, and therefore the ratio $\theta/\theta_0 = 2.5$ is greater than 1. We then expect the BG pulsed beam to be very similar to the limiting Bessel-*X* wave (see Sec. V B), which is shown in Fig. 2(b). The only significant difference is that the arms of the letter ''*X*'' of the BG pulsed beams are slightly damped.

Figure 3 illustrates the propagation of the BG pulsed beam away from $z=0$. After the time intervals $t = 13\,123$ and 26 246 fs, the BG pulsed beam arrives at $z = D/2$ and *D*, respectively [see Figs. 3(a) and 3(b)], where the diffraction-free range is $D = 7.875$ mm. It can be seen that the BG pulsed beam approximately preserves its initial form, except for the tendency to loosen the front arms and to increase the intensity of the rear arms. This peculiarity is due to the lateral displacement of the interfering ID pulses on propagation. In fact, at the time $t = z_0 \cos\theta/c$ [Fig. 3(c)], when the BG pulsed beam has propagated at the distance $z_0 = 18$ mm sizably larger than the diffraction-free range, the rear arms are almost splitted off from the partially obscured axial zone. Therefore, the pulsed beam acquires the form of an annulus, formed by the no longer overlapping ID pulses. The slight bending of the splitted rear arms reflects, in fact, the curvature of the pulse fronts of the ID pulses [3].

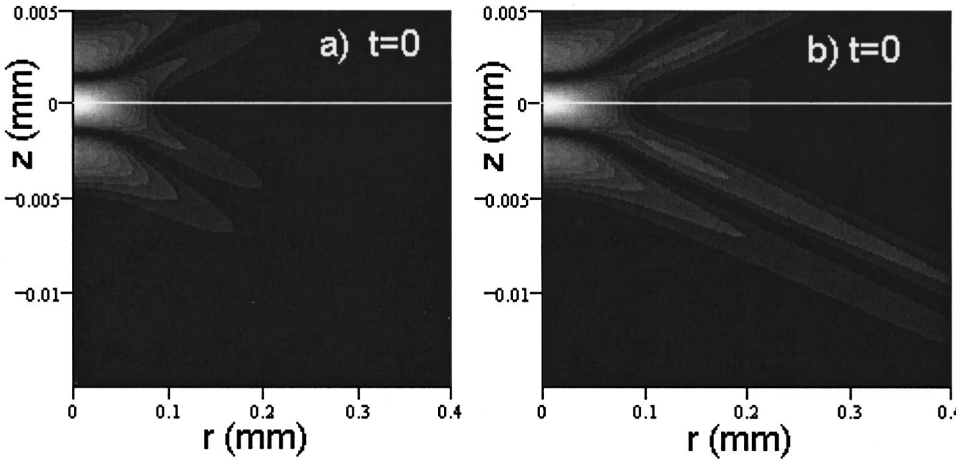

FIG. 2. Gray scale plots of the real field $|\mathrm{Re}\, E(r,z,t)|$ of (a) the BG pulsed beam defined by the parameters ($z_0=18$ mm, $\theta=0.025$ rad, $\alpha=6$, $t_0=18$ fs) and (b) the Bessel-X pulsed beam of parameters ($\theta=0.025$ rad, $\alpha=6$, $t_0=18$ fs).

As for the residual on-axis amplitude [Fig. 3(c)], some stretching and deceleration of the pulse is appreciated. It is of interest to verify this point from the general expression (17) of the BG pulsed beams. For on-axis points, Eqs. (13) and (17) reduce to

$$E(0,z,t)=\frac{iz_0}{q}F\left(t''-\frac{z^2\theta^2}{2cq}\right), \tag{32}$$

which can also be written in the form

$$E(0,z,t)=\frac{iz_0}{q}F\left(t''-\frac{z^3\theta}{2c|q|^2}+i\,\frac{z^2\theta^2 z_0}{2c|q|^2}\right). \tag{33}$$

This expression is to be compared with the invariable on-axis pulse form $F(t'')$ of the Bessel-X pulse. Apart from the overall amplitude change iz_0/q, we see that the pulse form of the BG pulsed beam shifts on propagation by a z-dependent complex quantity. The real part $z^3\theta^2/2c|q|^2$ of the shift is an actual time delay with respect to the X-Bessel wave, from which the pulse velocity at any propagation distance z can easily be evaluated to be

$$v(z)=\frac{c}{1-\dfrac{\theta^2}{2}(1-z^2/|q|^2)}. \tag{34}$$

Instead of the superluminal constant velocity $v=c/(1-\theta^2/2)\simeq c/\cos\theta$ of the Bessel-X waves, the velocity of the BG pulsed beam $v(z)$ ranges from the superluminal one $c/\cos\theta$ within the diffraction-free range down to c for large propagation distances. The imaginary part $z_0 z^2\theta^2/2c|q|^2$ of the shift amounts to a change in the pulse form on propagation, which may involve, depending on the specific choice of $F(t)$, pulse broadening, frequency shift, and deformation [3].

For example, the on-axis field of the BG pulsed beam with the Poisson-like spectrum, as given by Eqs. (25) and (26), can be displayed in the form

$$E(0,z,t)=\frac{iz_0}{q}\left(\frac{t_0}{t_0+z^2 z_0\theta^2/2c|q|^2}\right)^{\alpha}\times\left[\frac{i(t_0+z_0 z^2\theta^2/2c|q|^2)}{(t''-z^3\theta/2c|q|^2)+i(t_0+z^2 z_0\theta/2c|q|^2)}\right]^{\alpha}, \tag{35}$$

which shows that in this case the on-axis temporal form remains a Poisson-like spectrum function on propagation, but the scaling parameter t_0 is replaced with $t_0+z^2 z_0\theta^2/2c|q|^2$. This change results in an increasing pulse duration and a diminishing frequency of the oscillations upon propagation, which from Eqs. (22) and (23) are given by

$$T(z)=T+\left(\frac{2}{\alpha}\right)^{1/2}\left(\frac{z_0\theta^2}{2c}\right)\left(\frac{z}{|q|}\right)^2 \tag{36}$$

and

$$\omega_m(z)=\frac{\alpha}{t_0+(z_0\theta^2/2c|q|^2)z^2}, \tag{37}$$

respectively. A detailed analysis of these formulas shows that the pulse duration and frequency remain almost constant and equal to those of the Bessel-X wave within the diffraction-free range, and start to vary slowly outside that range up to the highest duration $T+\sqrt{1/\alpha}(z_0\theta^2/2c)$ and down to the smallest frequency $\alpha/(t_0+z_0\theta^2/2c)$ in the far field ($z\gg z_0$).

An approximate far-field expression of the pseudo-nondiffracting ($\theta\gg\theta_0$) BG pulsed beams of arbitrary pulse form can be obtained from the asymptotic form of Eq. (13) for $z\to\infty$, $r\to\infty$. For $z\gg z_0$ we can write $q\simeq z$, and for large r we can let $J_0(ix)=I_0(x)\sim\exp(x)/\sqrt{2\pi x}$, where $x=z\omega\theta r/zc$, $I_0(\,)$ is the zero-order, first kind, modified Bessel function [23], and we have used its asymptotic form for a large argument [30]. Equation (13) then becomes

$$E(r,z,t)\sim\frac{i}{z}\int_0^\infty d\omega\,\hat{f}(\omega)\left(\frac{z}{\omega r}\right)^{1/2}\exp\left[-\frac{\omega z_0}{2cz^2}(r-z\theta)^2\right]\times\exp\left[i\omega\left(t'-\frac{r^2}{2cz}\right)\right], \tag{38}$$

where unessential amplitude constants have been omitted. If $\theta>\theta_0$, the center $z\theta$ of the Gaussian function in the integrand is sizably larger than its width $\sqrt{2cz^2/\omega z_0}$. Therefore,

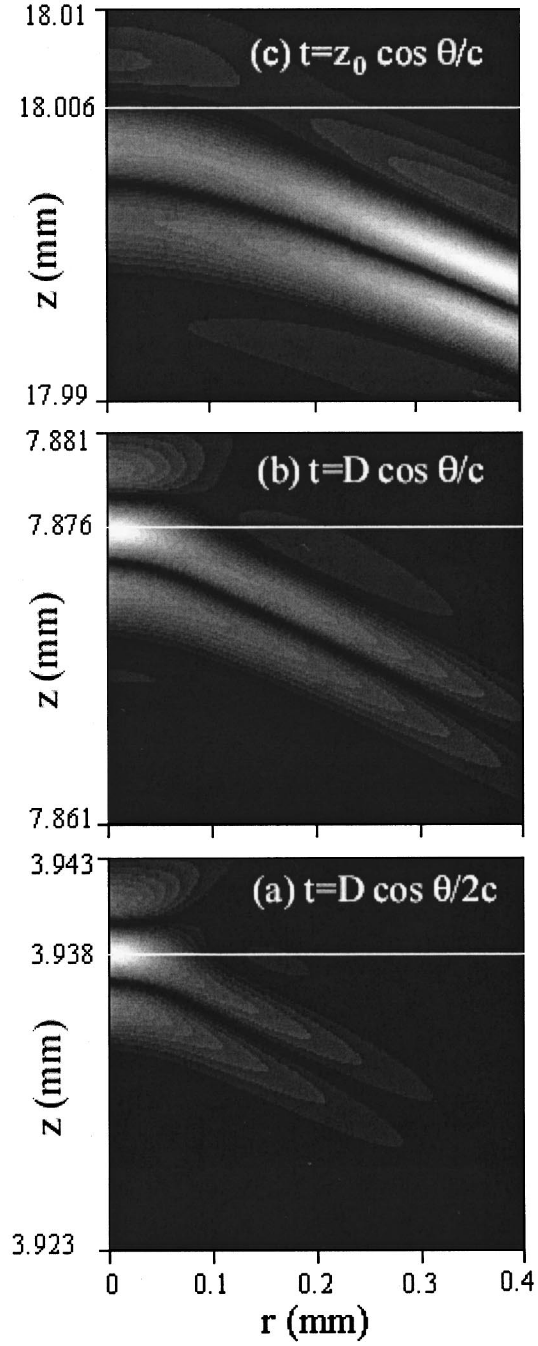

FIG. 3. Gray scale plots for the propagation of the BG pulsed beam of Fig. 2. The white horizontal lines indicate the positions of center of the superluminal Bessel-*X* pulse at the times indicated in each plot.

r in the square root can be replaced by its mean value within the Gaussian function, i.e., $r \simeq z\theta$. On doing so, we obtain

$$E(r,z,t) \sim \frac{i}{z}\int_0^\infty d\omega\, \frac{\hat{f}(\omega)}{\sqrt{\omega}} \exp\left[i\omega\left(t' - \frac{r^2}{2cz}\right)\right] \times \exp\left[-\frac{\omega z_0}{2cz^2}(r - z\theta)^2\right] \tag{39}$$

as an asymptotic expression of the BG pulsed beams with $\theta \gg \theta_0$ in the far field. The energy distribution

$$W(r,z) = \int_{-\infty}^{\infty} [\mathrm{Re}\, E(r,z,t)]^2 = \tfrac{1}{2}\int_{-\infty}^{\infty} |E(r,z,t)|^2 dt \tag{40}$$

can now be written, from Parseval's theorem, as

$$W(r,z) \sim \frac{1}{z^2}\int_0^\infty d\omega\, \frac{|\hat{f}(\omega)|^2}{\omega} \exp\left[-\frac{\omega z_0}{cz^2}(r - z\theta)^2\right]. \tag{41}$$

The form of this equation indicates that the transversal energy distribution $W(r,z=\text{const})$ takes a maximum at $r = z\theta$, and is a strictly decreasing function away from this maximum. On the other hand, the dependence of $E(r,z,t)$ on time through the quantity t' denotes that the on-axis pulse propagates at the velocity c in the far field, as we have seen above. In addition, the time delay $r^2/2cz$ of the arrival of the pulse at each plane z accounts for a spherical pulse front of radius z. In short, in the far field a pseudo-non-diffracting BG pulsed beam has the form of an annulus of mean radius $r = z\theta$ over the surface of an expanding sphere at the velocity of light c.

VII. RELATION WITH THE BESSEL-GAUSS PULSE OF OVERFELT

In the paraxial wave equation (2), the variables z' and t' play a symmetrical role. Then the interchange $z' \to ct'$, $t' \to z'/c$ in any solution results in a new solution. In particular,

$$E(r,z,t) = \frac{iz_0}{q}\left\{ \frac{it_0}{\left[(z_c/c + it_0)^2 - \left(\frac{iz_0}{cq}\theta r\right)^2\right]^{1/2}}\right\}^{\alpha} \times P_{\alpha-1}\left\{ \frac{z_c/c + it_0}{\left[(z_c/c + it_0)^2 - \left(\frac{iz_0}{cq}\theta r\right)^2\right]^{1/2}}\right\}, \tag{42}$$

where $q = ct' + iz_0$,

$$z_c = z'' - \frac{1}{2cq}(r^2 + \theta^2 c^2 t'^2), \tag{43}$$

and $z'' = z + ct'\theta^2/2$ is a solution of the wave equation under the paraxial approximation, which to our knowledge has not been previously reported. Its nature can be understood by writing Eq. (42) as

$$E(r,z,t) = \frac{iz_0}{q}\frac{1}{\pi}\int_0^\infty d\omega\, \hat{f}(\omega) \exp\left[-\frac{i\omega}{2cq}(r^2 + c^2 t'^2\theta^2)\right] \times J_0\left(\frac{iz_0}{q}\frac{\omega}{c}\theta r\right) \exp(i\omega z''/c), \tag{44}$$

where $\hat{f}(\omega)$ is again the Poisson-like spectrum, but the basis functions in the superposition are now

$$E(r,z,t)=\frac{iz_0}{q}\exp\left[-\frac{i\omega}{2cq}(r^2+c^2t'^2\theta^2)\right]$$
$$\times J_0\left(\frac{iz_0}{q}\frac{\omega}{c}\theta r\right)\exp(i\omega z''/c). \quad (45)$$

These functions are also solutions of the paraxial wave equation (2), and can be readily identified with the paraxial approximations to the BG focus wave modes, first described by Overfelt [31], and recently reconsidered in several works [32–34], namely,

$$E(r,z,t)=\frac{a_1}{V}J_0\left(\frac{\kappa a_1 r}{V}\right)\exp\left(-\frac{\beta r^2}{V}\right)$$
$$\times\exp\left(\frac{-i\kappa^2 a_1\xi}{4\beta V}\right)\exp(i\beta\eta), \quad (46)$$

where $\xi=z-ct$, $\eta=z+ct$, $V=a_1+i\xi$, and a_1, β, and κ are free parameters. In fact, on identifying $a_1=z_0$, $\beta=\omega/2c$, $\kappa=\omega\theta/c$, and neglecting backpropagating waves by approaching $\eta=z+ct\simeq 2z$, Eq. (46) becomes Eq. (45) after straightforward algebraic manipulations. Our Eq. (42) is then a superposition of these BG focus wave modes, in an analogous way that Ziolkowski's EDPET's [12] are superpositions of the fundamental Gaussian focus wave modes [35]. The detailed study of Eq. (42) is deferred to future work. We only point out here that Eq. (42) contains as particular cases of its free parameters most of the classes of focus wave modes previously known, as $(\theta=0)$ Ziolkowski's EDPET's with the Poisson-like spectrum [12], $(\theta=0,\alpha,t_0\to\infty,\alpha/t_0=\text{const})$ the original Brittingham focus wave mode [35], and $(\theta\neq 0,\alpha,t_0\to\infty,\alpha/t_0=\text{const})$ Overfelt's BG pulse.

VIII. CONCLUSIONS

We have studied few-cycle pulsed-beam solutions of the paraxial wave equation obtained by superposing BG beams of different frequencies but having the same Rayleigh range and cone angle as those produced by mode-locked resonators with toroidal mirrors, or equivalently, by superposing identical ID pulses with propagation directions distributed over the surface of a cone. In particular, we have found BG pulsed beams with the Poisson-like spectrum as a new solution of the paraxial wave equation in free space, representing spatially and temporally localized waves with finite energy and pseudo-non-diffracting behavior. Each pulsed beam is expressed in terms of a rational function and a Legendre polynomial, and is defined by the values of four parameters. Suitable choices of these parameters yield the ID and Bessel-*X* pulses, and in the many-cycle limit the BG beams and therefore the Gaussian and Bessel beams. The four-parameter, closed-form expression of the BG pulsed beams may be of interest as an alternative analytical representation of the above beams and pulsed beams for further analytical developments, or to synthesize new solutions of the wave equation on integrating over the free parameters.

BG pulsed beams satisfying the relation $\theta>\theta_0$ appear to be of particular interest. They are finite-energy replicas of the nondiffracting, nondispersing, superluminal Bessel-*X* waves within a finite propagation distance $2D$, this distance being larger than the equivalent diffraction length expected from their transversal size. Outside the diffraction-free range, the letter *X* starts deformating, breaking, and slowing down. At large propagation distances, the three-dimensional pulsed-beam structure is transformed into an expanding annulus propagating at the velocity of light c.

The reported pulsed beam can be easily generalized by superposing higher-order BG beams with vortices, or the more recently reported [36,37] generalized BG beams. In another sense, the study of the propagation of BG pulsed beams in dispersive media may also be of interest, since a suitable choice of frequency dependence of the cone angle of the Bessel beams composing an *X*-Bessel wave is known to result in the suppression or diminution of pulse spreading on propagation due to dispersion [38].

ACKNOWLEDGMENTS

The authors acknowledge the partial support of Ministerio the Educación y Cultura of Spain, Acción Integrada Hispano-Italiana HI-1998-0083, and of Ministero dell'Università e delle Ricerca Scientifica Italiano, Confinanziamento 9802109290_001. The authors thank Franco Gori for helpful discussions and making possible this collaboration.

[1] T. Brabec and F. Krausz, Rev. Mod. Phys. **72**, 545 (2000).
[2] A. E. Kaplan, J. Opt. Soc. Am. B **15**, 951 (1998).
[3] M. A. Porras, J. Opt. Soc. Am. B **16**, 1468 (1999).
[4] M. A. Porras, Phys. Rev. A **60**, 5069 (1999).
[5] T. Brabec and F. Krausz, Phys. Rev. Lett. **78**, 3282 (1997).
[6] S. Feng and H. G. Winful, J. Opt. Soc. Am. A **16**, 2500 (1999).
[7] E. Ibragimov, Appl. Opt. **34**, 7280 (1995).
[8] E. M. Belenov and A. V. Nazarkin, Pis'ma Zh. Eksp. Teor. Fiz. **53**, 188 (1991) [JETP Lett. **53**, 200 (1991)].
[9] E. M. Belenov and A. V. Nazarkin, J. Opt. Soc. Am. A **11**, 168 (1994).
[10] E. Heyman and L. B. Felsen, J. Opt. Soc. Am. A **6**, 806 (1989).
[11] M. A. Porras, Phys. Rev. E **58**, 1086 (1998).
[12] R. Ziolkowski, Phys. Rev. A **39**, 2005 (1989).
[13] A. T. Friberg, J. Fagerholm, and M. M. Salomaa, Opt. Commun. **136**, 207 (1997).
[14] J. Lu and J. F. Greenleaf, IEEE Trans. Ultrason. Ferroelectr. Freq. Control **39**, 441 (1992); **39**, 19 (1992).
[15] P. R. Stepanishen and J. Sun, J. Acoust. Soc. Am. **102**, 3308 (1997).
[16] S. Feng and H. G. Winful, Phys. Rev. E **61**, 862 (2000).
[17] J. Durnin, J. Miceli, Jr., and J. H. Eberly, Phys. Rev. Lett. **15**, 1499 (1987).
[18] C. J. R. Sheppard and T. Wilson, Microwaves, Opt. Acoust. **2**, 105 (1978).
[19] F. Gori, G. Guattari, and C. Padovani, Opt. Commun. **64**, 491 (1987).
[20] P. Pääkkönen and J. Turunen, Opt. Commun. **156**, 359 (1998).
[21] C. Altucci, R. Bruzzese, D. D'Antuoni, C. de Lisio, and S.

Solimeno, J. Opt. Soc. Am. B **17**, 34 (2000).

[22] C. F. R. Caron and R. M. Potvliege, J. Opt. Soc. Am. B **15**, 1096 (1998).

[23] M. Abramowitz and I. A. Stegun, *Handbook of Mathematical Functions* (Dover, New York, 1972).

[24] Z. Jiang, Opt. Commun. **125**, 207 (1996).

[25] Z. Jiang, Q. Lu, and Z. Liu, Appl. Opt. **34**, 7183 (1995).

[26] Y. Wang, Q. Chen, and Q. Y. Xu, Opt. Commun. **157**, 93 (1998).

[27] J. K. Jabczynski, Opt. Commun. **77**, 292 (1990).

[28] P. D. Einziger and S. Raz, J. Opt. Soc. Am. A **4**, 3 (1987).

[29] Abdul-Azeez R. Al-Rashed and Bahaa E. A. Saleh, Appl. Opt. **34**, 6819 (1995).

[30] I. S. Gradstein and I. M. Ryzhik, *Tables of Integrals, Series, and Products* (Academic, New York, 1965).

[31] P. L. Overfelt, Phys. Rev. A **44**, 3941 (1991).

[32] P. L. Overfelt, J. Opt. Soc. Am. A **14**, 1087 (1997).

[33] P. L. Overfelt, J. Opt. Soc. Am. A **16**, 2239 (1999).

[34] V. V. Borisov and I. I. Simonenko, Can. J. Phys. **75**, 573 (1997).

[35] J. N. Brittingham, J. Appl. Phys. **54**, 1179 (1983).

[36] V. Bagini, F. Frezza, M. Santarsiero, G. Schettini, and G. Schirripa, J. Mod. Opt. **43**, 1155 (1996).

[37] M. Santarsiero, Opt. Commun. **132**, 1 (1996).

[38] H. Sonajalg, M. Rtsep, and P. Saari, Opt. Lett. **22**, 310 (1997).